ORIGINAL PAPER

Nitrogen limitation in eucalypt roots: a cascading influence on the mobilization of soil organic matter

Luis Carlos Colocho Hurtarte[1] · Ivan Francisco Souza[2] · Rodrigo Teixeira Ávila[3] · Luís Fernando J. Almeida[2] · Gabriela Soares[2] · Leonardus Vergütz[4] · Ivo Ribeiro Silva[2]

Abstract

Emerging scientific evidence has shown that root exudates may trigger the mobilization of soil organic matter (SOM), particularly under nutrient limitation. However, the role of changes in root morphology, metabolism, exudation, and their impact on rhizospheric properties and SOM remain poorly known. To address this issue, we conducted a rhizobox experiment for 50 days in which pre-grown eucalypt plants (120 days-old) were supplied with nutrient solutions providing either limited (0.0 mg L^{-1}) or normal N supply (196.0 mg L^{-1}). After 48 days, we used a $^{13}CO_2$ pulse labeling to track the impact of N limitation on C translocation to roots and soil respiration. After the 50th day, we assessed root morphology and metabolism, rhizospheric pH, mineral crystallinity, C and N contents, and the molecular composition of SOM. Under N limitation, eucalypt plants showed reduced photosynthesis, increased their root-to-shoot ratio and root branching, with organic acids prevailing among root metabolites. Overall, N-limited eucalypt plants led to a cascading of changes in the rhizosphere: increased concentrations of recently fixed ^{13}C-CO_2, citrate, and N-bearing compounds, whereas soil pH and Fe-bound SOM decreased. These results were not followed by significant changes in microbial biomass, neither fungi: bacteria nor Gram-positive: Gram-negative ratios. Our results show that under N limitation, eucalypt roots exhibited a cascade of morpho-physiological adjustments that ultimately increased the mobilization of some SOM pools. Therefore, the combined impacts of those root morpho-physiological traits on the mobilization of SOM may reduce the overall soil C sink of eucalypt forests under N limitation.

Keywords Rhizosphere · Nitrogen · ^{13}C-CO_2 distribution · Tropical soil · Rhizobox

Introduction

Emerging scientific evidence has drawn worldwide attention to the relevance of root exudation on soil respiration, particularly in a scenario of global rise in atmospheric CO_2 (Heimann and Reichstein 2008; Jilling et al. 2018; Ainsworth and Long 2020). Increasing concentration of atmospheric CO_2 could boost C_3 photosynthesis rates, which in turn could lead to an increased demand for plant nutrients (Terrer et al. 2018; Ainsworth and Long 2020). Among these nutrients, special consideration should be given to nitrogen (N), whose stocks and mineralization rates strongly depend on soil organic matter (SOM) dynamics (Jilling et al. 2018; Henneron et al. 2020; Gan et al. 2022). Some studies have stressed that root exudates may accelerate the mobilization and the mineralization of SOM (Keiluweit et al. 2015), whereas other studies have emphasized the central role of root exudates among the major precursors driving SOM formation (Sokol and Bradford 2018). Therefore, considering the mineralization or formation of soil C pools is important.

Several strategies can be deployed by plants to overcome short- or long-term limitations in soil nutrient availability. For instance, under limited N supply plants may increase belowground C allocation, boost fine root biomass

✉ Ivan Francisco Souza
ivanfrsouza@gmail.com; ivan.souza@ufv.br

[1] Diamond Light Source, Harwell Science and Innovation Campus, Didcot OX11 0DE, UK

[2] Departamento de Solos, Universidade Federal de Viçosa, Viçosa 36570-900, Minas Gerais, Brazil

[3] Departamento de Fisiologia Vegetal, Universidade Federal de Viçosa, Viçosa 36570-900, Minas Gerais, Brazil

[4] Chair of Soil Science, Mohammed VI Polytechnic University (UM6P), Benguerir 43150, Morocco

production and augment exudation rates (Chen et al. 2010; Phillips et al. 2011; Meier et al. 2020; Sun et al. 2021). These adjustments can occur in tandem with increasing branching and root specific length, both of which could increase the soil volume to be explored (Liese et al. 2017; Meier et al. 2020). Therefore, roots morpho-physiological changes could reflect an intensification of "nutrient foraging", whose impacts on SOM mobilization and/or mineralization remain uncertain. Moreover, owing to the spatiotemporal complexity of rhizospheric processes, most studies consider only total plant C allocation belowground under nutrient limitation, with less consideration given to variations in root morphology or exudate chemistry (Högberg et al. 2001; Wenzel et al. 2001). Hence, constraining how root morpho-physiology may be adjusted by plants growing under limited N availability as well as their overall impacts in the rhizosphere.

Changes in root morpho-physiological traits are often linked to increased microbial growth and enzyme activity in the rhizosphere (Phillips et al. 2011). As such, root exudation could provide energy (e.g., sugar) to stimulate soil microbes that in turn would mobilize and degrade SOM as typically referred to as 'rhizospheric priming' effects (Grayston et al. 1997; Kuzyakov et al. 2000; Meier et al. 2017). Another proposed mechanism for SOM mobilization by exudates is the release of chelating organic acids (e.g., oxalate) that are able to disrupt mineral-organic associations (Keiluweit et al. 2015). Nonetheless, the role of these processes in soil under plants growing limited by soil N availability remains unclear. It remains poorly understood whether plants growing under limited N supply could alter the chemical composition of their exudates specifically to stimulate microbial activity or whether changes in exudate chemistry are simply a consequence of plant metabolism under N limitation.

The main objective of this study was to evaluate the effect of N supply level on the mobilization of SOM by investigating (i) root morphological traits and exudates, (ii) changes in soils properties (i.e., pH, total C and N contents, concentration of organic acids in the soil solution, and soil respiration), and finally (iii) changes in the molecular composition of SOM and rhizospheric main microbial groups. To achieve these goals, we cultivated pre-grown (120 days-old) eucalypt plants in a controlled experiment for 50 days.

Materials and methods

Soil sampling and experimental set-up

For this study, soil was sampled in an area that had been cultivated with a tropical grass species (*Brachiaria decumbens* (*Trin.*) *Griseb.*) over the last 20 years in Paula Cândido,

Minas Gerais – Brazil (20° 52' S, 42° 58' E). After sampling, the soil was air-dried and sieved in a 2-mm mesh screen; it is a Haplic Ferralsol (IUSS Working Group WRB 2015) with loamy texture, pH_{H2O} of 5.24, total organic C (TOC) and total N (TN) contents about 25.4 and 1.4 g kg^{-1} soil, respectively (C: N about 18:1). Our experimental units consisted of a rhizobox system designed by Wenzel et al. (2001), modified to include a CO_2 sampler (Supplementary Figure S1). This system included two physically separated vertical compartments: an upper compartment containing washed sand (> 0.05 mm < 2 mm) in which the plants were cultivated and a lower compartment containing 189.0 g of dry soil (bulk density about 1.2 g cm^{-3}). We also adjusted and kept the moisture content fixed at 200.0 mg g^{-1} soil, equivalent to 70.0% of the water holding capacity (0.342 cm^3 cm^{-3}). By using the rhizobox system we could control the supply of nutrients to the plants without adding nutrients directly to the soil. The upper compartment had a narrow slit on its bottom, through which the roots could penetrate the lower compartment. Within the lower compartment, the contact between the roots and the soil was limited by a nylon membrane with a pore size of 5.0 μm (Tegape, Brazil). The lower compartment also had a soil-air probe, which consisted of a coiled silicone rubber tube about 20.0 cm long, with a 5.0 mm internal diameter connected to a 15.0 cm copper tube that crossed through and projected out of the upper compartment (Kammann et al. 2001). We kept the tube assembled closed by a three-way stopcock that was only opened during the sampling of the soil air within the lower compartment of the rhizobox (Supplementary Figure S2).

Plant growth experiment

Our experiment was arranged according to a complete factorial scheme including the following two factors: The first factor was the plant effect, thus the rhizoboxes were assembled either without plants (-Plant) or with plants (+Plant); The second factor was N fertilization, for which we used an incomplete modified Clark's solution (Clark 1982) without N (-N) or with N (+N) supply by a nutrient solution containing a N concentration of 7.0 mmol L^{-1} (i.e., 196.0 mg L^{-1}) with 50% as NO_3^- and 50% as NH_4^+ as shown in Supplementary Table S1. These nutrient solutions were kept in plastic vessels and applied through capillarity into the upper compartment using the glass fiber wicks. In total, we had 12 experimental units with three replicates.

The experimental units were incubated in a growth chamber to control the photon flux (~340.0 μmol cm^{-2}), temperature (25 °C) and air humidity (60%). In the upper compartment, we planted clonal seedlings of a eucalypt hybrid (*Eucalyptus grandis* W. Hill ex Maiden) x *Eucalyptus urophylla* S. T. Blake), approximately 120 days old.

During the first 20 days after planting, all roots remained in the upper compartment of the rhizobox. Each rhizobox was wrapped up in aluminum foil and subsequently placed inside a 30.0 L black polyethylene box to avoid light disturbance to the roots and to prevent algae/moss growing within the rhizosphere. We grew the plants for 30 days after the roots started to penetrate in the lower compartment, totaling 50 days after planting until the end of the experiment.

After the 48th day of the plant growth, we placed all intact rhizoboxes into an acrylic chamber (448 dm^3 volume) and submitted to a pulse-labeling with ^{13}C-CO_2 by dissolving ^{13}C-CO_3 with a diluted solution of HCl (Machado et al. 2011). In total, the duration of the isotope labeling was 16 h. At the end of the following day (i.e., 50th day after the experiment began), the SPAD index of mature leaves was measured using a Chlorophyll meter SPAD-502Plus (Konica Minolta – Japan). Samples of the soil air were taken through the soil-air probe (Supplementary Figure S2) using a 5-mL syringe and transferred into previously evacuated 12-mL vials, and analyzed for CO_2 concentration and their $^{13}C/^{12}C$ ratio relative to the Vienna-Pee-Dee Belemnite (PDB) internal standard by an Isotopic Ratio Mass Spectrometer- IRMS (ANCA-GSL, 20–20, Sercon, Crewe, UK). Subsequently, we took pictures of the root mat formed within the lower compartment before harvesting the plants.

Upon harvesting, the roots grown in the lower compartment were immediately freeze-dried under N_2 and kept in an ultra-freezer at -80 °C until further analysis. Finally, the rhizoboxes were opened and the soil moisture was measured by a sensor (EC-5, Decagon, Pullman, WA). Afterwards, the soil within the lower compartment was sectioned in three distances parallel to the root mat (0–3 mm, 3–6 mm and 6–15 mm) with a microtome (Fitz et al. 2003). These samples were further split; the soil solution was extracted from one subsample through centrifugation according to Pérez et al. (2002); the other soil subsample was freeze-dried and stored until further analysis. The shoot material was collected and separated into 'old' and 'new' tissues reflecting plant materials grown before and after the beginning of the experiment, respectively. These tissues were dried under forced air circulation at 65 ± 2 °C, weighed, milled, and kept in airtight boxes at 4 °C until further analysis. Total C, N, and isotopic content of the plant tissues were analyzed by the IRMS as described above.

Chemical analyses

The extracted soil solution was freeze-dried, solubilized with 1.0 mL of ultra-pure water and filtered through a 0.45 µm membrane. An aliquot (0.5 mL) was diluted up to 2.0 mL with ultra-pure water and analyzed for citric and oxalic acids by ion exchange chromatography (Silva et al.

2004). The pH of the freeze-dried soil samples was analyzed in water according to Pansu and Gautheyrou (2006). SOM fractions were obtained through a physical fractionation (Cambardella and Elliott 1992), by dispersing 3.0 g of soil in a sodium hexametaphosphate solution (1.0 g L^{-1}) using a soil: solution ratio of 1:3. The soil slurry obtained was wet-sieved using 53-µm mesh screen to obtain SOM with particle-size higher and smaller than 53 µm. Hereafter, we refer to the SOM in the particle-size fraction < 53 µm as mineral-associated organic matter (MAOM) (Lavallee et al. 2018). These two particle-size fractions were dried under forced air circulation at 50 °C and kept in airtight boxes at 4 °C until further analysis. We determined TOC and TN contents and their respective $^{13}C/^{12}C$ and $^{15}N/^{14}N$ ratios of the MAOM fraction using the IRMS described above. We also assessed changes in short-range-order (SRO) minerals and organic bound Fe and Al oxyhydroxides in the MAOM fraction according to Pansu and Gautheyrou (2006) by using oxalate and pyrophosphate extractions, respectively. After these extractions, we used atomic absorption spectrometry (Agilent Technologies 200 Series AA Model 240 FS, Santa Clara, CA, USA) to determine the concentration of Al and Fe released from the samples (Shang and Zelazny 2015).

Root analyses

We used the Gia Roots software to evaluate the pictures of the roots (Galkovskyi et al. 2012). In this procedure, the cropping tool of the software selected the areas of roots and the scale was manually defined. We chose all parameters used in root identification for each photo individually using the double adaptive image thresholding to include (i) the average root diameter, (ii) the root area, (iii) the root length, (iv) the surface area and (v) the specific root length. The composition of metabolites produced by the roots grown in the lower compartment was determined following a chromatographic method as proposed by Lisec et al. (2006). Briefly, 100.0 mg of the root tissues frozen under liquid nitrogen were immediately frozen-grinded and extracted with 1.4 mL of methanol. For quantification, we used 60.0 µL of internal standard (0.2 mg ribitol mL^{-1} water). This mixture (root extract and internal standard) was mixed vigorously with 1.4 mL of water for 15 min at 70 °C. We added 750.0 µL of chloroform to the mixture to separate polar and nonpolar metabolites. All compounds were identified by their mass spectra and their retention time index was compared to the mass spectral collection of the NIST11 database. Quantitative analyses were based on the peak height values of the recorded mass feature and calculated for the dry weight of each subsample and by the response of the internal standard from each respective GC-MS chromatogram to obtain normalized results.

Changes in organic matter and minerals in soil samples from different distances of the rhizoplane

We determined changes in the molecular chemistry of the organic compounds within the MAOM fraction by using off-line tetramethyl ammonium hydroxide (TMAH) mediated by thermochemolysis (Del Rio et al. 1998). All TMAH-thermochemolysis products were analyzed by gas chromatography-mass spectrometry in a Shimadzu QP 2010-SE GC-MS equipped with a Rtx – 5MS column (30 m length; 0.25 mm ID; 0.25 μm film thickness), using ultra-pure He as the carrier gas at a flow rate of 3 mL min^{-1}, the temperature of the ion source was set to 200 °C, the temperature of the interface was set to 290 °C and oven temperature increased from 60 up to 300 °C at a rate of 15 °C min^{-1}. We identified all eluted compounds in the chromatograms using the NIST 2011 mass spectral library and standard compounds.

To assess changes in crystalline soil minerals during the plant growth phase and evaluate changes in the composition of SOM through its thermal degradation, we used synchrotron X-ray diffraction (XRD) analysis coupled to evolved gas analysis by mass spectrometry (EGA-MS) at the XPD-10B beamline (Ferreira et al. 2006) of the Brazilian Synchrotron Light Laboratory (LNLS). Briefly, 100.0 mg of the MAOM fraction of each treatment (soil layers from 0 to 3 mm and 3–6 mm distances from the rhizoplane) were heated from room temperature up to 500 °C, while XRD data was collected by coupling an "Anton Paar XRK900" furnace to the beam end station and heating the sample, under an air flow of 150 mL^{-1} min (80% He, 20% O$_2$) at a heating rate of 5.0 °C min^{-1}. During the heating period we collected XRD patterns between 10 and 50 °2θ. Simultaneously, all gases evolved from the samples were collected and analyzed by a coupled mass spectrometer (QMA 200 – Pfeiffer-Vacuum) for ions with m/z 17 and 18 (OH and H$_2$O), 27 (HCN), 28 (CO), 30 (NO), 44 (CO$_2$ and N$_2$O) and 46 (NO$_2$).

We used the software Peakfit® to analyze the EGA-MS data for H$_2$O and CO$_2$ by adjusting modified Gaussian functions for signal deconvolution and area calculation. Our XRD data was analyzed using the Fytik 0.9.8, with an initial polynomial background subtraction applied to the diffraction patterns, and the subsequent identification of the main recorded peaks. Changes in the crystalline structure of iron and aluminum (hydr)oxides and clay minerals were assessed by considering variations in the main peaks using Lorentzian functions and assessing their centroid and width.

Phospholipid fatty acids (PLFA) analysis

Phospholipids fatty acids were determined in each of the three soil layers (0–3 mm, 3–6 mm and 6–15 mm). Upon their collection, samples were immediately stored in containers at −80 °C. We extracted and separated the PLFAs according to the procedure described by Butler et al. (2003) and we profiled main microbial groups as described by Willers et al. (2015) and Tavi et al. (2013). We assigned Gram-positive bacterial biomass to the fatty acids i15:0, a15:0, i16:0, and i17:0; Gram-negative bacteria using the fatty acids cy17:0 and cy19:0 (Joergensen 2022). We calculated total bacterial PLFAs by summing gram-positive and gram-negative bacterial fatty acids as well as of the fatty acid 16:1ω7 (Frostegård et al. 1993; Joergensen 2022). Fungal biomass included both saprotrophic fungi and ectomycorrhizal biomass and we used the fatty acids 18:2ω6 (Federle et al. 1990; Joergensen 2022).

Statistical analysis

We tested the assumptions for normality and homogeneity of variances by using Kolmogoroff-Smirnoff test and Levene's test, respectively. Total aboveground biomass production, root dry matter yield, root traits and soil CO$_2$ concentrations were tested using a F-test ($p < 0.05$). Changes in soil physicochemical properties as a function of the distance from the root plane were tested using a two-way ANOVA followed by Dunnett-test ($p < 0.05$). These analyses were performed using the STATISTICA software (Statsoft Inc.).

Results

Changes in plant growth and metabolism in response to N availability

Generally, the plants grown under N limitation showed the leaf SPAD index of 27.3, approximately 33.9% lower than those receiving normal N supply plants ($p < 0.05$; Table 1). N-deficient plants also produced almost 41.0% less shoot biomass, although both N-limited and N-supplied plants

Table 1 Leaf-$_{SPAD\ Index}$, new shoot and root dry matter yield and root: shoot ratio of Eucalypt seedlings as affected by N supply

Parameter	N supply via nutrient solution (196.0 mg L^{-1})		N supply via nutrient solution (0.0 mg L^{-1})	
	Shoot	Root	Shoot	Root
Leaf-$_{SPAD\ Index}$	41.33 ± 1.76 a	-	27.33 ± 1.20 b	-
Dry mass (g)	2.01 ± 0.14 a	0.42 ± 0.04 A	1.19 ± 0.04 b	0.41 ± 0.02 A
Root: Shoot	0.21 ± 0.02 b		0.35 ± 0.05 a	

Values are means ± standard error ($n = 3$). Means followed by the same letter do not differ at $p < 0.05$ (F-test)

Table 2 Root traits estimated at the end of the experimental period for eucalypt plants grown under distinct N-supply computed by the Gia Roots Software

Root traits	N supply via nutrient solution (196.0 mg L^{-1})	N supply via nutrient solution (0.0 mg L^{-1})	p-value
Average diameter (mm)	3.77 A	2.84 A	0.087
Root length (cm)	900.64 B	1814.34 A	0.049
Root surface area (cm^2)	94.36 B	178.69 A	0.031

Values are means ($n = 3$). Means followed by the same letter do not differ at $p < 0.05$ (F-test)

showed similar total root biomass (0.41 g and 0.42 g, respectively). As a result, the root: shoot ratio was 0.35 for N-deficient and 0.21 for N-supplied plants ($p < 0.05$; Table 1). Under N limitation, the roots exhibited several morphological changes (Supplementary Figure S3), which led to higher root length and specific surface area ($p < 0.05$) and comparatively lower root diameter ($p < 0.087$) than the plants receiving normal N supply (Table 2).

As expected, both old and new shoot tissues of the plants grown under normal N supply showed higher N content and lower C: N ratios than those submitted to N limitation ($p < 0.05$; Table 3). Both old and new shoot tissues grown under normal N supply showed N contents about 3.3 and 4.2 times higher than those under N limitation ($p < 0.05$). Consequently, the C: N ratios of old and new shoot tissues under normal N supply were approximately 35 and 27:1, respectively. In contrast, these respective C: N ratios were 117 and 118:1 for the plants grown under N limitation ($p < 0.05$; Table 3). Unlike shoot tissues, neither the total N content nor the C: N ratios of the roots were significantly affected by the differential N supply ($p > 0.05$; Table 3). As such, the respective C: N ratios of old and new shoot tissues were about 3.4 and 4.4 higher under N limitation as compared to their N-supplied counterparts. For roots under N limitation, their C: N ratio was only about 1.5 higher than those grown under normal N supply (Table 3).

Our results suggest that the influence of N availability on root morphology (Tables 1 and 2, Supplementary Figure S3) and affected the total N contents of the plant tissues and their C: N ratios (Table 3) likely influencing the overall root metabolism (Fig. 1).

Accordingly, the relative abundance of amino acids (e.g., proline, leucine, glutamine, threonine, asparagine,

and tyrosine) and amines (e.g., phenylethanolamine, ethanolamine) were considerably reduced under N limitation (Fig. 1). In addition, plants growing without N addition also showed less sugars (e.g., maltose, fructose, cellobiose, glyceric acid) than those receiving normal N supply. Curiously, the only N-bearing compounds that increased under N limitation were phenylalanine and hydroxylamine. In contrast, N limitation favored the synthesis/accumulation of many low-molecular weight organic acids (e.g., citric, oxalic, malic) (Fig. 1), all of which were much less abundant in roots grown under normal N supply.

We did not observe significant differences among the treatments neither for the measurements of CO_2 concentration nor the $\delta^{13}C$-CO_2 by the end of the plant growth experiment (Fig. 2).

On average, the CO_2 concentration of the control plots without plant and no N supply (-Plant -N) was about 857.9 mg L^{-1} and about 1,133.0 mg L^{-1} for those without plants receiving normal N supply (-Plant + N, Fig. 2A). Generally, the averaged CO_2 concentration reached 1,241.0 mg L^{-1} in the treatment with plants without N fertilization (+ Plant -N), whereas for the N-supplied counterpart (+ Plant + N) this average was about 944.2 mg L^{-1} (Fig. 2A). Furthermore, the isotopic signature of the CO_2 released in these respective treatments was approximately + 700.0 and + 300.0‰ (Fig. 2B). This data shows a relatively short timeframe between the incorporation of ^{13}C in photosynthesis, the transfer of ^{13}C-labeled products to roots and their release as $^{13}CO_2$.

Changes in properties of the soil samples from different distances of the rhizoplane

By moving along the three distances from the rhizoplane (i.e., 0–3 mm) towards the bulk soil volume (i.e., 3–6, and 6–15 mm), some soil chemical and physicochemical properties significantly changed due to the presence of the plants and the differential N supply (Fig. 3). The total organic C content of the MAOM fraction decreased in the 0–3 mm distance from the rhizoplane in the presence of plants ($p < 0.05$; Fig. 3). In contrast, the N content of the MAOM fraction of the treatment under N limitation increased about 5.0% relative to the control without plants receiving normal N supply ($p < 0.05$; Fig. 3). Instead, there was a decrease in the N

Table 3 Total C and N content, and C: N ratios of shoot (old and new) and roots tissues of N-supplied and N-deficient eucalyptus seedlings. The letters compare the differences in mean C and N contents and C: N ratio between N supplied and N deficient plant shoot (old and new) and roots

N supply level	N supply via nutrient solution (196.0 mg L^{-1})			N supply via nutrient solution (0.0 mg L^{-1})		
Tissue	C, g kg^{-1}	N, g kg^{-1}	C: N	C, g kg^{-1}	N, g kg^{-1}	C: N
Old shoot	424.6 A	12.4 A	34.7 B	439.3 A	3.8 B	116.9 A
New Shoot	426.7 A	16.1 A	26.6 B	449.0 A	3.8 B	118.0 A
Roots	408.5 A	10.6 A	44.0 A	415.0 A	6.2 A	68.5 A

Values are means ($n = 3$). Means followed by the same letter do not differ at $p < 0.05$ (F-test)
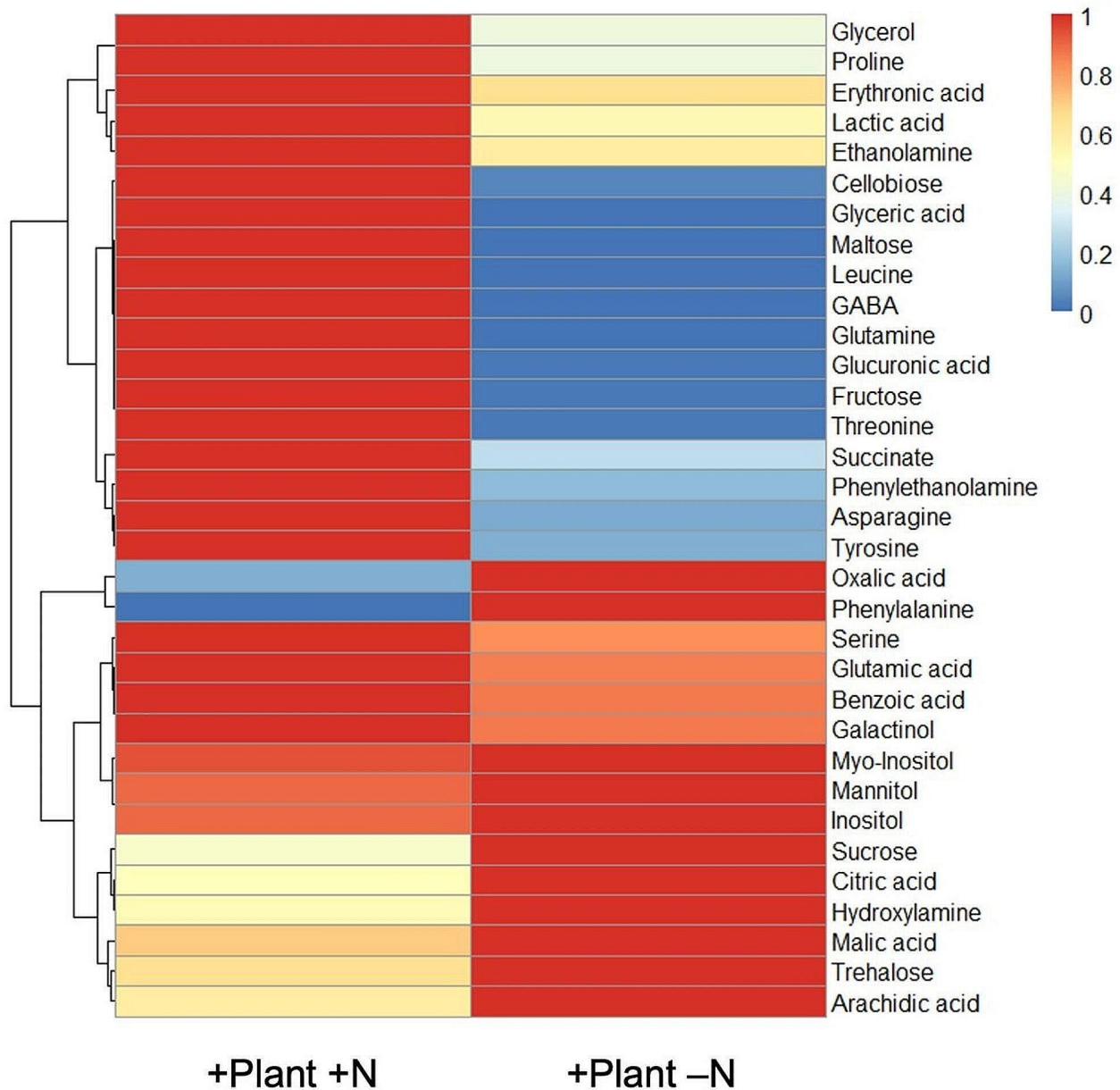
Fig. 1 Heatmap depicting the normalized abundance of root metabolites as a function of the distinct N supply via nutrient solution; +Plant + N: eucalypt plants receiving normal N supply (196.0 mg L^{-1}); +Plant -N: eucalypt plants receiving no N addition (0.0 mg L^{-1})

content of about 7.0% in the treatment receiving normal N supply within the 0–3 mm distance from the rhizoplane relative to the control without plants receiving normal N supply ($p < 0.05$; Fig. 3). These changes in C and N contents were followed by a significant reduction in the oxalate-extractable Fe, but only for the plants grown under N limitation ($p < 0.05$, Fig. 3).

No significant change was observed in oxalate extractable Al for the treatments with plants (without or with N supply) relative to the control without plants (Fig. 3). Concurrently, the plants grown under N limitation showed a

marked increase in the concentration of citrate in the soil solution (between 60 and 200%) over the entire 0–15 mm distance from the rhizoplane relative to the control without plants ($p < 0.05$; Fig. 3). Likewise, the pH of the soil solution also decreased about −0.5 units across the entire distance from the rhizoplane (0–15 mm) of the plants under N limitation ($p < 0.05$; Fig. 3). For the plants receiving normal N supply, the pH of the soil solution decreased only within the first 3 mm from the rhizoplane (Fig. 3). Moreover, the increase in citrate in the soil solution mirrored a significant ^{13}C enrichment of the MAOM fraction for the distance
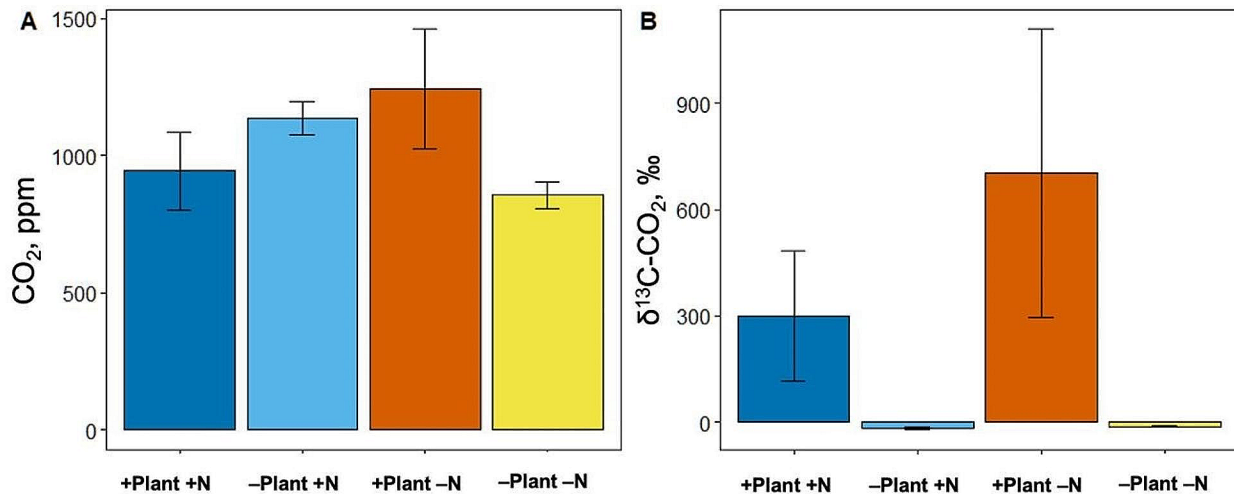
Fig. 2 Mean CO_2 concentrations (**A**) and its δ^{13}C-CO_2 (per mil, ‰) signature (**B**) released from the intact rhizoboxes measured 16 h after a pulse with ^{13}C enriched CO_2, that is at the end of the plant growth experiment. Description: +Plant + N: eucalypt plants receiving normal N supply (196.0 mg L^{-1}); -Plant + N: control without eucalypt plants receiving normal N supply (196.0 mg L^{-1}); +Plant -N: eucalypt plants receiving no N addition (0.0 mg L^{-1}); -Plant -N: control without eucalypt plants receiving no N addition (0.0 mg L^{-1}). Values are means ± standard error ($n = 3$). There were no significant differences among the treatments ($p > 0.05$)

between 0 and 3 mm from the rhizoplane, particularly in the treatments with plants under N limitation (Supplementary Table S2; $p < 0.05$). The second and third layers i.e., 3–6 and 6–15 mm, did not show detectable ^{13}C enrichment of the MAOM fraction (Supplementary Table S2 $p > 0.05$).

Responses of main microbial groups to the presence of plants and N availability

We also examined the composition of the main microbial groups across the three distances from the rhizoplane, i.e., 0–3, 3–6, and 6–15 mm (Fig. 4). Although there were variations in the fungal-to-bacterial (F: B) ratio and for the GP: GN ratio in the treatments and across the distances considered (Fig. 4), those changes were not statistically significant. This trend was also observed for distance between 3 and 6 mm from the root plane (Fig. 4). It can be inferred that despite the significant changes observed in root morphology (Table 1), exudate composition (Fig. 1) and rhizosphere chemistry (Fig. 3) owing to the distinct N availability to eucalypt plants, these changes did not affect the composition main soil microbial groups as indicated in Fig. 4.

Synchrotron-based XRD and EGA-MS

We evaluated the changes in crystalline soil minerals by using synchrotron-based XRD and assessed the thermal degradation of the MAOM fractions of samples collected within 0–3 and 3–6 mm from the rhizoplane by EGA-MS.

Generally, we observed no changes in the d-spacing nor in the full width at half maximum (FWHM) of the main peaks of kaolinite and gibbsite, regardless of the presence of plants or N supply. However, we observed a decrease in the d-spacing and the FWHM for the main peak of goethite in the treatment with plants under N limitation relative to the treatments with N-supplied plants. As such, the d-spacing for the 101 hkl plane showed a slight decrease from 0.4149 to 0.4131 nm and the FWHM were about 0.732 and 0.531 (º2θ) in the respective treatments (Supplementary Table S3). The d-spacing of goethite in the controls without plants were about 0.4158 nm (no N addition) and 0.4153 (normal N supply), and their peaks showed the same FWHM (0.826) as shown in Supplementary Table S3.

Relative to the controls without plants, the MAOM fraction from both planted treatments showed a similar decrease in CO_2 evolution from the samples collected within the 0–3 mm layer during the thermal degradation (Table 4). The reduction in CO_2 release during the temperature interval between 0 and 155 °C was about 32–37% and 13–15% between 320 and 550 °C (Table 4; Supplementary Figure S4-S5). However, for the temperature interval between 320 and 550 °C, only those with plants grown without N addition also released less CO_2 (24%), whereas the samples receiving normal N supply released only 3% less CO_2 than the control (without plants and no N supply). Furthermore, for the samples collected in the second layer (3–6 mm from the rhizoplane), only the samples from the treatments with plants grown without N addition showed consistently lower
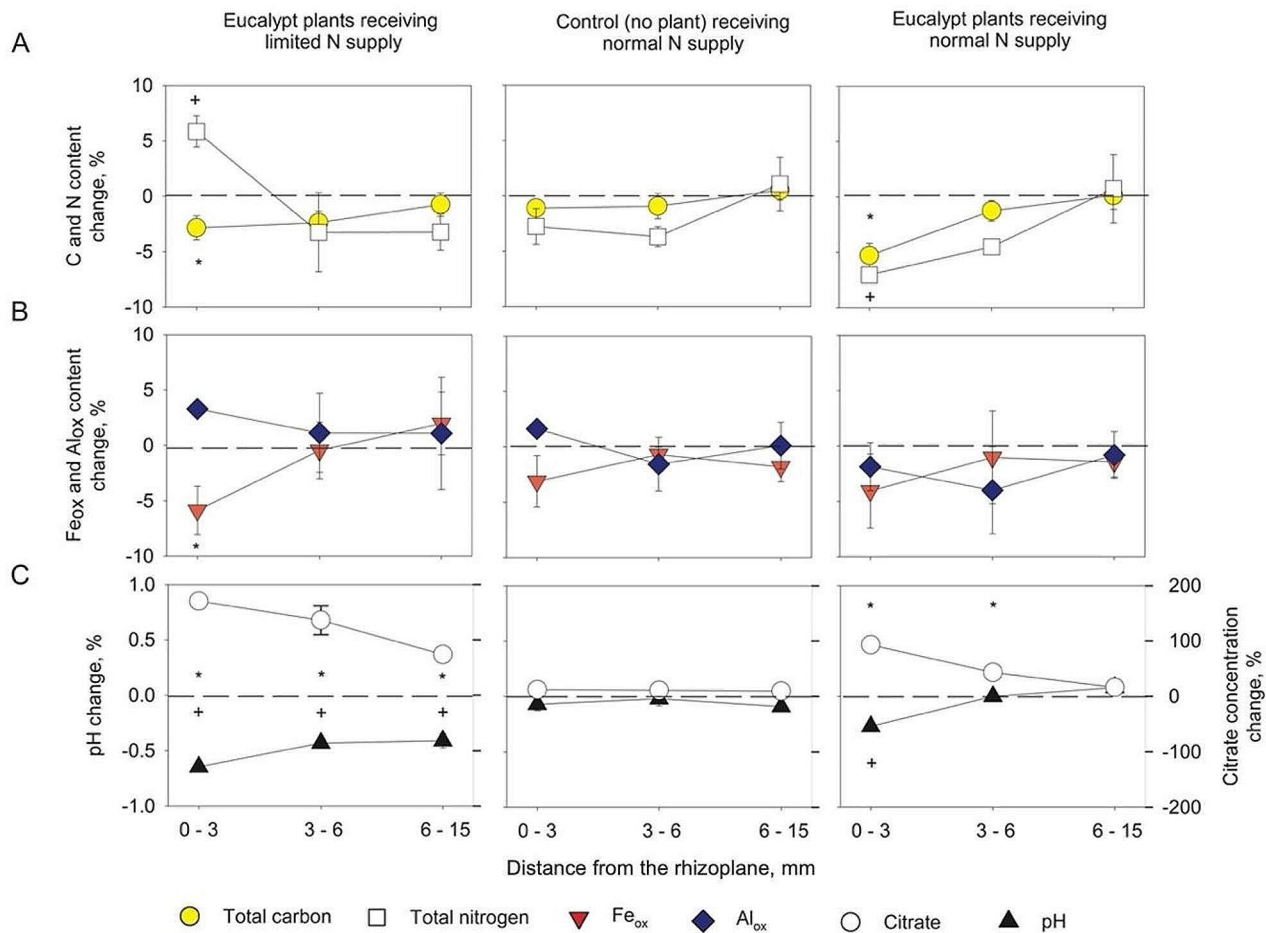
Fig. 3 Percentual (%) changes in soil properties under eucalypt plants treated with a nutrient solution with a limited (0.0 mg L^{-1}) N supply of N (left) or with a normal (196.0 mg L^{-1}) N supply (right) relative to the control with neither plants nor N supply (dashed line). The control without plants receiving normal N supply is shown in the center panel. Soil properties evaluated included (**A**) soil C and N content; (**B**) iron and aluminum extracted by oxalate (Fe$_{ox}$ and Al$_{ox}$) from the mineral-associated organic matter (MAOM) fraction (i.e., soil particle-size fraction smaller than 53 μm) and (**C**) pH (left axis) and citrate in the soil solution (right axis). Significant differences for a given treatment with eucalypt plants relative to the treatment without eucalypt plants receiving no N addition (dashed line) are indicated by asterisks (two-way ANOVA, followed by Dunnet's test $p < 0.05$). Values are means ± standard error ($n = 3$)

CO_2 evolution than the control treatment for temperatures between 0 and 155 and 155–320 (Table 4).

Changes in molecular structure of the MAOM fraction of the three soil layers sampled at different distances of the rhizoplane

According to our off-line TMAH-GC/MS, aliphatic such as long-chain alcohols and alkanes were the most abundant constituents of the extracted MAOM fraction.

Generally, the abundance of aliphatic materials decreased in the first soil layer from the rhizoplane (0–3 mm) in the treatment with plants grown without N addition (Fig. 5), whereas the relative proportion of N-bearing compounds increased (Fig. 5). In contrast, for the second and third soil layers (3–6 and 6–15 mm), the differences between the treatments were less evident. By considering all three layers (0–15 mm) the relative abundance of cutin- and suberin-derived compounds did not change, and aromatics and suberin-derived compounds accounted for a small fraction of the extracted materials (Fig. 5). A list with the major chemical groups identified is given in the Supplementary Table S4, whereas all compounds identified in our TMAH-GC/MS of the three layers (i.e., 0–3, 3–6 and 6–15 mm) are listed in the Tables S5, S6 and S7.

Discussion

Root morphology and metabolism in response to N limitation

According to previous studies on woody plants such as eucalypt, the concentration of N in their leaf and root
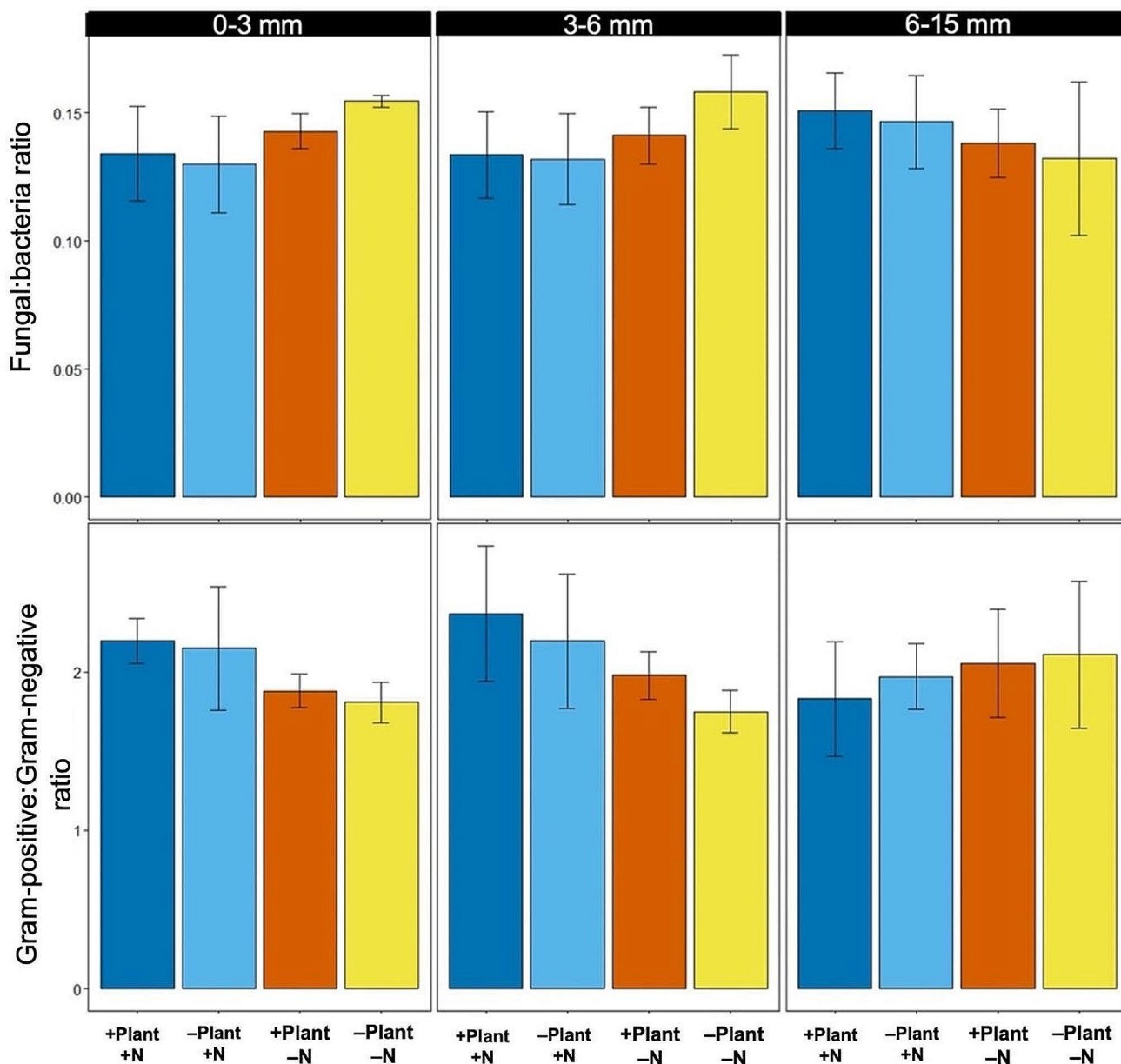
Fig. 4 Fungal: bacteria (F: B) ratio and Gram-positive: Gram nega-tive bacterial ratio of each soil layer as inferred from the phospholipid fatty acids (PLFA) profiling. +Plant+N: eucalypt plants receiving normal N supply (196.0 mg L^{-1}); -Plant+N: control without eucalypt plants receiving normal N supply (196.0 mg L^{-1}); +Plant -N: eucalypt plants receiving no N addition (0.0 mg L^{-1}); -Plant+N: control with-out eucalypt plants receiving no N addition (0.0 mg L^{-1}). There were no significant differences among the treatments ($p > 0.05$). Values are means ± standard error ($n = 3$)

Table 4 Relative changes in CO_2 (m/z 44) evolution from the mineral-associated organic matter (MAOM) fraction (i.e., soil particle-size fraction smaller than 53 μm) of the treatments with eucalypt receiving distinct levels of N fertilization via nutrient solution Percentages (%) are measured changes relative to the CO_2 evolution of the unplanted non-fertilized (–Plant –N) control

Treatment description	+Plant +N	+Plant –N	+Plant +N	+Plant –N
Temperature Range, °C	0–3 mm		3–6 mm	
0–155	–32	–37%	+14	–16%
155–320	–15%	–13%	–9	–19%
320–500	–3	–24%	6%	0%

+Plant+N: eucalypt plants receiving normal N supply (196.0 mg L^{-1}); -Plant+N: control without eucalypt plants receiving normal N supply (196.0 mg L^{-1}); +Plant -N: eucalypt plants receiving no N addition (0.0 mg L^{-1}); -Plant+N: control without eucalypt plants receiving no N addition (0.0 mg L^{-1}). Values are means ($n = 3$)
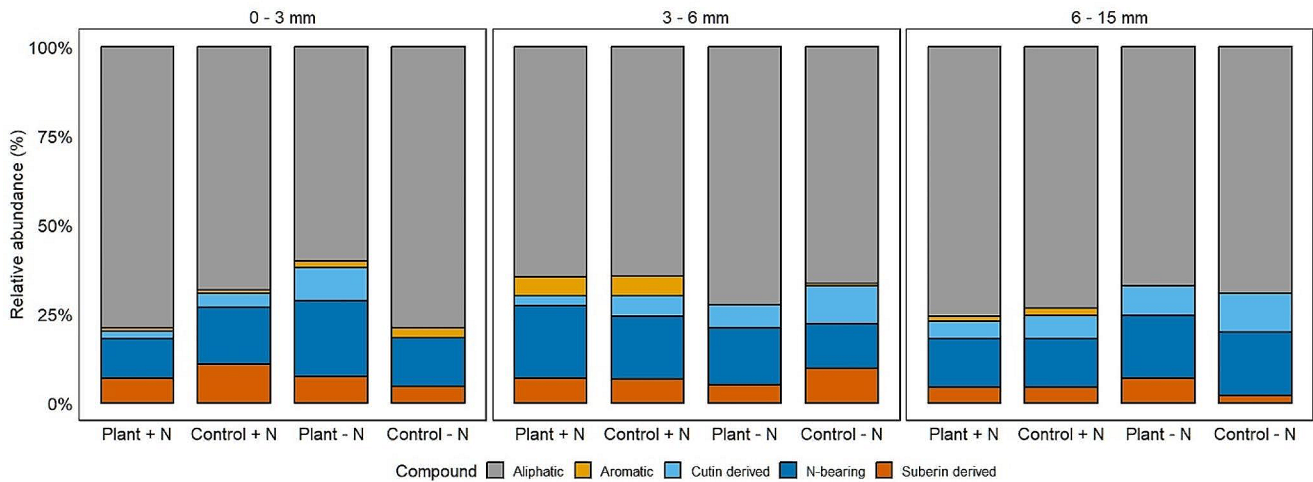
Fig. 5 Relative abundance (%) of chemical groups (aliphatics, aromatics, cutin-derived, N-bearing, and suberin-derived compounds) extracted from the mineral-associated organic matter (MAOM) fraction (i.e., soil particle-size fraction smaller than 53 μm) as a function of the distance from the rhizoplane in the rhizobox (0–3, 3–6 and 6–15 mm from the root plane. +Plant+N: eucalypt plants receiving normal N supply (196.0 mg L^{-1}); -Plant+N: control without eucalypt plants receiving normal N supply (196.0 mg L^{-1}); +Plant -N: eucalypt plants receiving no N addition (0.0 mg L^{-1}); -Plant+N: control without eucalypt plants receiving no N addition (0.0 mg L^{-1}). Significant differences among the treatments for each distance from the rhizoplane are given in Supplementary Table S4. Values are means ($n=3$)

tissues should be positively correlated (Valverde-Barrantes et al. 2017). Hence, as inferred from the SPAD index (Table 1), eucalypt plants grown without N addition showed a decreased shoot growth in favor of root growth and morphological changes. Possibly, the N-limited plant invested proportionally more resources to increase root branching and consequently increase root specific surface area (Table 2). Morphological changes shown by roots under N limitation can be interpreted as a strategy by the plant to explore a larger volume of soil and/or favor interactions with rhizospheric microbiome (Weemstra et al. 2016; Liese et al. 2017; Moreau et al. 2019; Bergmann et al. 2020). According to our PLFA analysis, the soil microbiome was dominated by bacteria and both F: B and GP: GN ratios were not substantially affected by the treatments (Fig. 4). Therefore, rather than impacting composition of the main microbial groups, changes in root morphology under N limitation may reflect the effort of the plants to directly explore the surrounding rhizospheric soil (Ostonen et al. 2007; Bergmann et al. 2020; Wang et al. 2023). Nonetheless, an increased effort by the plants themselves to augment the soil volume explored could inevitable affect microbial activity and the potential mobilization of nutrients from SOM (Sterkenburg et al. 2018). Another likely outcome associated to increased rates of root branching could be the direct transfer of senescing root tissues, mucilage, and exudates to form new soil C pools (Lavallee et al. 2018). Hence, under the paradigm that roots are more efficient to form SOM than aboveground plant litter (Jackson et al. 2017), those morphological changes indicated in Table 2 could be interpreted

as strongly favorable to the transfer of root-derived C into SOM pools.

Beyond altered morphological traits, our results also showed a significant change in root metabolism under N limitation, particularly a reduction in the concentration of amino acid and N-bearing compounds among root metabolites, except for phenylalanine (Fig. 1). Poplars (*Populus* × *canescens* (Ait.) Smith) supplied with phenylalanine showed increased root production as compared to plants supplied with NH$_4$NO$_3$ (Jiao et al. 2018). Additionally, some poplar species treated with phenylalanine showed increased N use efficiency (Hu et al. 2020). Probably, the high content of phenylalanine in eucalypt roots under N limitation may reflect adjustments in their metabolism linked to those changes observed in morphological traits (Table 2). Moreover, we observed an increase in the concentration of organic acids, some sugars (e.g., sucrose and trehalose), and sugar alcohols (i.e., inositol, mannitol, and myo-inositol) among the main metabolic products of roots grown under N limitation (Fig. 1). To some extent, the accumulation of organic acids may be due to the limited N supply and a decrease in the synthesis of amino acids (Carvalhais et al. 2011). The release of exudates (e.g., organic acids, sugars) in the rhizosphere may stimulate microbial growth and activity (Sasse et al. 2018), which in turn could accelerate the mineralization of nutrients that can be taken up by plants (Bergmann et al. 2020; Gan et al. 2022; Wang et al. 2023). Although our isotopic data showed a fast transfer of C from shoots to the roots (Fig. 2), it is not possible to distinguish the CO$_2$ released directly by root respiration from the CO$_2$ released upon the microbial assimilation of root-derived

materials in the rhizosphere. Nonetheless, considering the changes in root morphology observed under limited N supply, it is likely that most of the isotopically labeled CO_2 released in our experiment was derived from root respiration as evidenced in previous studies on this subject (Jia et al. 2013; Rewald et al. 2014; Paradiso et al. 2019). All these studies highlighted a strong relationship between fine root biomass and root respiration. Thus, the presumed primacy of root exudation for the buildup of SOM pools (Sokol and Bradford 2018) coupled to a larger volume of soil in direct contact with root tissues and exudates (Lavallee et al. 2018), might favor soil C storage where eucalypt plants are grown under low N availability.

Changes in the rhizosphere under N limitation

Our results indicate that the soil solution of the rhizosphere of eucalypt plants grown under N limitation showed low pH and high concentration citrate that probably led to the mobilization of N-rich materials from the MAOM, especially Fe-bound pools (Figs. 3 and 5). A conceptual diagram showing these cascading effects derived from N limitation is given in Fig. 6.

Besides, considering that the soil used in the lower compartment of the rhizobox had a C:N ratio about 18:1, a short-term microbial N immobilization likely occurred (Dijkstra et al. 2009; Bengtson et al. 2012). Additionally, it is relevant to point out that all changes in eucalypt root morphophysiological traits were not followed by significant changes in the composition of the main soil microbial groups (Fig. 4).

Generally, the impacts of root exudation on SOM formation as well as on its mobilization and mineralization remain controversial. For instance, some authors claim that the rhizospheric microbiome is highly efficient in assimilating root exudates (e.g., glucose) and subsequently transferring the assimilated C into the MAOM pool (Sokol and Bradford 2018; Teixeira et al. 2024). In contrast, Keiluweit et al. (2015) showed that chemical characteristics of the exudates (i.e., glucose, acetic acid, or oxalic acid) have different impacts on soil microbiome and SOM mineralization, with SOM mineralization being the highest in the presence of oxalic acid (low energy supply) and the lowest with glucose (high energy supply). In our study, the concentration of organic acids and some sugars among root metabolites increased under N limitation (Fig. 1), so the mixture of these compounds in the rhizosphere (i.e., citrate) could have
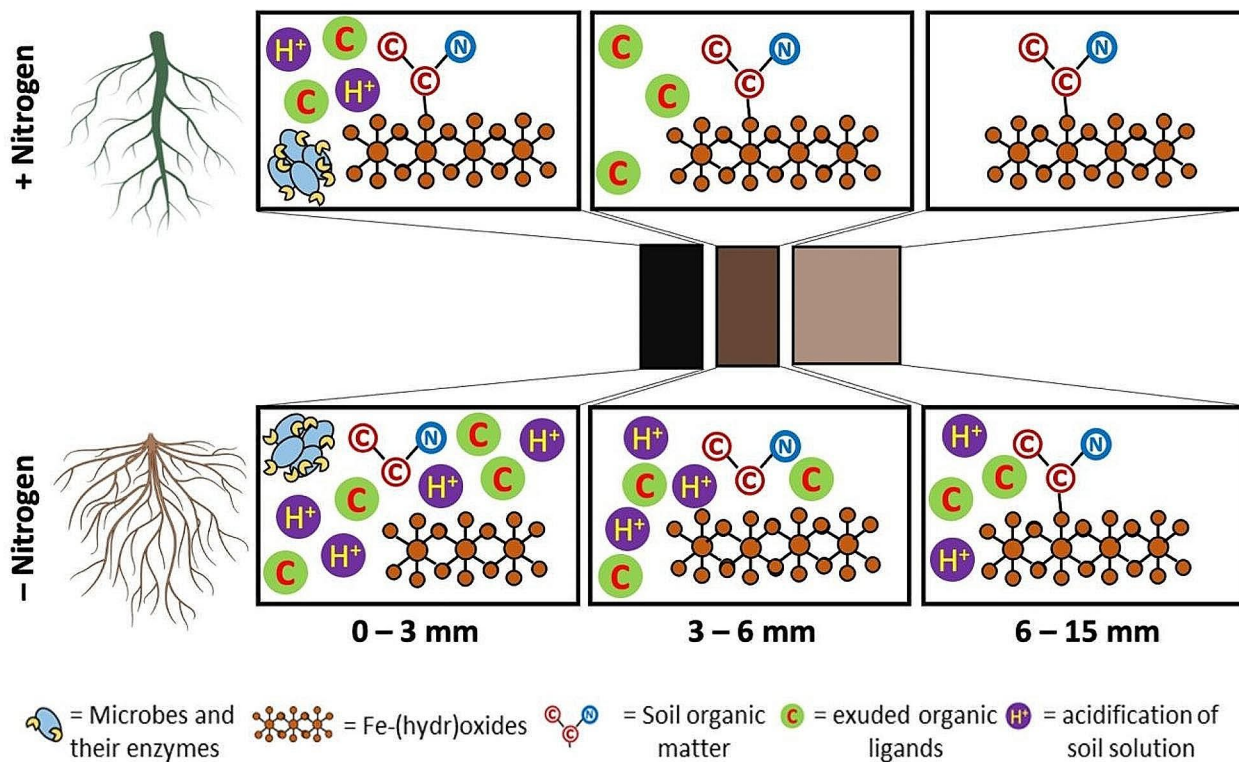

Fig. 6 Relative to the normal N supply (i.e., 196.0 mg L^{-1}), the rhizosphere of eucalypt plants grown under limited N availability (i.e., 0.0 mg L^{-1}) showed higher citrate concentration and lower pH (H^+) in the three soil layers (i.e., 0–3, 3–6 and 6–15 mm) from the rhizo-plane. Moreover, the acidification of the rhizosphere was followed by a significant reduction in Fe-bound organic materials and an increase in N-bearing organics in the soil solution of the first soil layer from the rhizoplane (i.e., 0–3 mm)

affected the relative stability of MAOM pools as well as provided energy (sugars) to boost microbial activity. Further, our data indicates a decrease in Fe-bound SOM in the first 0–3 mm from the rhizoplane (Figs. 3 and 6), coupled to the increased levels of citrate in the rhizosphere, and the acidification of the three soil layers evaluated under N limitation (Fig. 3). Thus, our results are in line with those reported by Keiluweit et al. (2015), despite this compared results obtained from natural and artificial exudates.

Although our root metabolomics showed increased synthesis of oxalic acid under N limitation (Fig. 1), we could not identify this compound in the rhizospheric soil. Possibly, the acidification of the rhizosphere might have caused the dissolution of poorly crystalline Fe minerals (i.e., Fe_{ox}) and some forms of goethite (as inferred from its d-spacing and FWHM) under N limitation (Supplementary Table S3). Subsequently, organic acids such as oxalic acid might have complexed the Fe derived from those minerals, whereas N-bearing compounds previously bound to Fe could have been released in the rhizosphere (Fig. 5), particularly within the first layer (i.e., 0–3 mm) from the rhizoplane.

As proposed in our conceptual model shown in Fig. 6, N limitation might lead to substantial changes in root morphology of eucalypt plants and alterations in the chemical properties of the rhizosphere. Once released in the rhizosphere, root exudates could directly disrupt mineral-organic associations and stimulate microbial activity, both of which could increase CO_2 emissions from soils (Heimann and Reichstein 2008; Bengtson et al. 2012; Keiluweit et al. 2015).

Conclusion

Overall, despite the increased contact between living root tissues and the rhizosphere soil coupled to high exudation rates, N limitation may not necessarily boost soil C storage. On the opposite, any external factor leading to limited soil N availability or increased demand of N by plants (e.g., increasing concentration of atmospheric CO_2) might favor net C losses from SOM. The acidic exudates released in the rhizosphere might act directly on the mobilization of mineral-protected SOM pools and/or boosting microbial activity, hence increasing total soil respiration rates. As such, we observed a relative increase in the concentration of N and a reduced concentration of C in MAOM fraction of the rhizosphere of the plants grown under N limitation, and a relatively fast release of CO_2 derived from recently fixed C atoms. Owing to the limited micro-environment in rhizobox-based approaches, future studies are warranted to include more complex soil systems. In complement, it is also critical to design and implement long-term evaluations to probe the interdependence among rhizosphere processes, soil C storage and turnover, and N cycling. Advancing our knowledge on these processes should depend largely on the assessment of their relationships with both composition and activity of the rhizosphere soil microbiome.

Author contributions Conceptualization: L.C.C.H; Methods: L.C.C.H, R.T.Á, L.F.A, G.S; Formal analysis and investigation: L.C.C.H, I.F.S; Writing - original draft preparation: L.C.C.H Writing - review and editing: L.C.C.H, I.F.S; Funding acquisition: I.R.S, L.V Resources: I.R.S; Supervision: I.R.S. All authors read and approved the paper.

Data availability Data will be made available upon request.

Declarations

Competing interest The authors declare that the research was conducted in the absence of any commercial or financial relationships that could be construed as a potential conflict of interest.

References

Ainsworth EA, Long SP (2020) 30 years of free-air carbon dioxide enrichment (FACE): what have we learned about future crop productivity and its potential for adaptation? Glob Chang Biol 27:1–23. https://doi.org/10.1111/gcb.15375

Bengtson P, Barker J, Grayston SJ (2012) Evidence of a strong coupling between root exudation, C and N availability, and stimulated SOM decomposition caused by rhizosphere priming effects. Ecol Evol 2:1843–1852. https://doi.org/10.1002/ece3.311

Bergmann J, Weigelt A, van der Plas F, Laughlin DC, Kuyper TW, Guerrero-Ramirez N, Valverde-Barrantes OJ, Bruelheide H, Freschet GT, Iversen CM, Kattge J, McCormack ML, Meier IC, Rillig MC, Roumet C, Semchenko M, Sweeney CJ, van Ruijven J, York LM, Mommer L (2020) The fungal collaboration gradient dominates the root economics space in plants. Sci Adv 6:eaba3756. https://doi.org/10.1126/sciadv.aba3756

Butler JL, Williams MA, Bottomley PJ, Myrold DD (2003) Microbial community dynamics associated with rhizosphere carbon

flow. Appl Env Microbiol 69:6793–6800. https://doi.org/10.1128/AEM.69.11.6793-6800.2003

Cambardella CA, Elliott ET (1992) Particulate soil organic-matter changes across a grassland cultivation sequence. Soil Sci Soc Am J 56:777–783. https://doi.org/10.2136/sssaj1992.03615995005600030017x

Carvalhais LC, Dennis PG, Fedoseyenko D, Hajirezaei MR, Borriss R, von Wirén N (2011) Root exudation of sugars, amino acids, and organic acids by maize as affected by nitrogen, phosphorus, potassium, and iron deficiency. J Plant Nutr Soil Sci 174:3–11. https://doi.org/10.1002/jpln.201000085

Chen D, Zhou L, Rao X, Lin Y, Fu S (2010) Effects of root diameter and root nitrogen concentration on in situ root respiration among different seasons and tree species. Ecol Res 25:983–993. https://doi.org/10.1007/s11284-010-0722-2

Clark R (1982) Nutrient solution growth of sorghum and corn in mineral nutrition studies. J Plant Nutr 5:1039–1057. https://doi.org/10.1080/01904168209363037

Del Rio JC, McKinney DE, Knicker H, Nanny MA, Minard RD, Hatcher PG (1998) Structural characterization of bio- and geo-macromolecules by off-line thermochemolysis with tetramethyl-ammonium hydroxide. J Chromatogr A 823:433–448. https://doi.org/10.1016/S0021-9673(98)00268-4

Dijkstra FA, Bader NE, Johnson DW, Cheng W (2009) Does accelerated soil organic matter decomposition in the presence of plants increase plant N availability? Soil Biol Biochem 41:1080–1087. https://doi.org/10.1016/j.soilbio.2009.02.013

Federle TW, Ventullo RM, White DC (1990) Spatial distribution of microbial biomass, activity, community structure, and the biodegradation of linear alkylbenzene sulfonate (LAS) and linear alcohol ethoxylate (LAE) in the subsurface. Microb Ecol 20:297–313. https://doi.org/10.1007/BF02543885

Ferreira FF, Granado E, Carvalho W Jr, Kycia SW, Bruno D, Droppa R Jr. (2006) X-ray powder diffraction beamline at D10B of LNLS: application to the Ba_2FeReO_6 double perovskite. J Synchrotron Rad 13:46–53. https://doi.org/10.1107/S0909049505039208

Fitz WJ, Wenzel WW, Wieshammer G, Isteniĉ B (2003) Microtome sectioning causes artifacts in rhizobox experiments. Plant Soil 256:455–462. https://doi.org/10.1023/A:1026173613947

Frostegård Å, Bååth E, Tunlio A (1993) Shifts in the structure of soil microbial communities in limed forests as revealed by phospholipid fatty acid analysis. Soil Biol Biochem 25:723–730. https://doi.org/10.1016/0038-0717(93)90113-P

Galkovskyi T, Mileyko Y, Bucksch A, Moore B, Symonova O, Price CA, Topp CN, Iyer-Pascuzzi AS, Zurek PR, Fang S, Harer J, Benfey PN, Weitz JS (2012) GiA roots: Software for the high throughput analysis of plant root system architecture. BMC Plant Biol 12:116. https://doi.org/10.1186/1471-2229-12-116

Gan D, Zeng H, Zhu B (2022) The rhizosphere effect on soil gross nitrogen mineralization: a meta-analysis. Soil Ecol Lett 4:144–154. https://doi.org/10.1007/s42832-021-0098-y

Grayston SJ, Vaughan D, Jones D (1997) Rhizosphere carbon flow in trees, in comparison with annual plants: the importance of root exudation and its impact on microbial activity and nutrient availability. Appl Soil Ecol 5:29–56. https://doi.org/10.1016/S0929-1393(96)00126-6

Heimann M, Reichstein M (2008) Terrestrial ecosystem carbon dynamics and climate feedbacks. Nature 451:289–292. https://doi.org/10.1038/nature06591

Henneron L, Kardol P, Wardle DA, Cros C, Fontaine S (2020) Rhizosphere control of soil nitrogen cycling: a key component of plant economic strategies. New Phytol 228:1269–1282. https://doi.org/10.1111/nph.16760

Högberg P, Nordgren A, Buchmann N, Taylor AFS, Ekblad A, Högberg MN, Nyberg G, Ottosson-Löfvenius M, Read DJ (2001) Large-scale forest girdling shows that current photosynthesis drives soil respiration. Nature 411:789–792. https://doi.org/10.1038/35081058

Hu Y, Li C, Jiang L, Liang D, Zhao X (2020) Growth performance and nitrogen allocation within leaves of two poplar clones after exponential and conventional nitrogen applications. Plant Physiol Biochem 154:530–537. https://doi.org/10.1016/j.plaphy.2020.06.053

IUSS Working Group WRB (2015) World Reference Base for soil resources 2014, update 2015. International soil classification system for naming soils and creating legends for soil maps. World soil resources reports No 106. FAO, Rome

Jackson RB, Lajtha K, Crow S, Hugelius G, Kramer MG, Piñeiro G (2017) The ecology of soil carbon: pools, vulnerabilities, and biotic and abiotic controls. Annu Rev Ecol Evol Syst 48:419–445. https://doi.org/10.1146/annurev-ecolsys-112414-054234

Jia S, McLaughlin NB, Gu J, Li X, Wang Z (2013) Relationships between root respiration rate and root morphology, chemistry and anatomy in *Larix gmelinii* and *Fraxinus mandshurica*. Tree Physiol 33:579–589. https://doi.org/10.1093/treephys/tpt040

Jiao Y, Chen Y, Ma C, Qin J, Nguyen THN, Liu D, Gan H, Ding S, Luo ZB (2018) Phenylalanine as a nitrogen source induces root growth and nitrogen-use efficiency in *Populus × canescens*. Tree Physiol 38:66–82. https://doi.org/10.1093/treephys/tpx109

Jilling A, Keiluweit M, Contosta AR, Frey S, Schimel J, Schnecker J, Smith RG, Tiemann L, Grandy AS (2018) Minerals in the rhizosphere: overlooked mediators of soil nitrogen availability to plants and microbes. Biogeochemistry 139:103–122. https://doi.org/10.1007/s10533-018-0459-5

Joergensen RG (2022) Phospholipid fatty acids in soil—drawbacks and future prospects. Biol Fertil Soils 58:1–6. https://doi.org/10.1007/s00374-021-01613-w

Kammann C, Grünhage L, Jäger HJ (2001) A new sampling technique to monitor concentrations of CH_4, N_2O and CO_2 in air at well-defined depths in soils with varied water potential. Eur J Soil Sci 52:297–303. https://doi.org/10.1046/j.1365-2389.2001.00380.x

Keiluweit M, Bougoure JJ, Nico PS, Pett-Ridge J, Weber PK, Kleber M (2015) Mineral protection of soil carbon counteracted by root exudates. Nat Clim Change 5:588–595. https://doi.org/10.1038/nclimate2580

Kuzyakov Y, Friedel J, Stahr K (2000) Review of mechanisms and quantification of priming effects. Soil Biol Biochem 32:1485–1498. https://doi.org/10.1016/S0038-0717(00)00084-5

Lavallee JM, Conant RT, Paul EA, Cotrufo MF (2018) Incorporation of shoot versus root-derived ^{13}C and ^{15}N into mineral-associated organic matter fractions: results of a soil slurry incubation with dual-labelled plant material. Biogeochemistry 137:379–393. https://doi.org/10.1007/s10533-018-0428-z

Liese R, Alings K, Meier IC (2017) Root branching is a leading root trait of the plant economics spectrum in temperate trees. Front Plant Sci 8:1–12. https://doi.org/10.3389/fpls.2017.00315

Lisec J, Schauer N, Kopka J, Willmitzer L, Fernie AR (2006) Gas chromatography mass spectrometry-based metabolite profiling in plants. Nat Protoc 1:387–396. https://doi.org/10.1038/nprot.2006.59

Machado DN, Novais RF, Silva IR, Loureiro ME, Milagres JM, Soares EMB (2011) Enriquecimento E alocação De ^{13}C em plantas de eucalipto. Rev Bras Ciênc Solo 35:857–866. https://doi.org/10.1590/S0100-06832011000300020

Meier IC, Finzi AC, Phillips RP (2017) Root exudates increase N availability by stimulating microbial turnover of fast-cycling N pools. Soil Biol Biochem 106:119–128. https://doi.org/10.1016/j.soilbio.2016.12.004

Meier IC, Tückmantel T, Heitkötter J, Müller K, Preusser S, Wrobel TJ, Kandeler E, Marschner B, Leuschner C (2020) Root exudation of mature beech forests across a nutrient availability gradient: the role of root morphology and fungal activity. New Phytol 226:583–594. https://doi.org/10.1111/nph.16389

Moreau D, Bardgett RD, Finlay RD, Jones DL, Philippot L (2019) A plant perspective on nitrogen cycling in the rhizosphere. Funct Ecol 33:540–552. https://doi.org/10.1111/1365-2435.13303

Ostonen I, Püttsepp Ü, Biel C, Alberton O, Bakker MR, Lõhmus K, Majdi H, Metcalfe D, Olsthoorn AFM, Pronk A, Vanguelova E, Weih M, Brunner I (2007) Specific root length as an indicator of environmental change. Plant Biosyst 141:426–442. https://doi.org/10.1080/11263500701626069

Pansu M, Gautheyrou J (2006) Handbook of soil analysis: mineralogical, organic and inorganic methods. Springer-, Berlin, Heidelberg

Paradiso E, Jevon F, Matthes J (2019) Fine root respiration is more strongly correlated with root traits than tree species identity. Ecosphere 10:e02944. https://doi.org/10.1002/ecs2.2944

Pérez DV, De Campos RC, Brevilato Novaes H (2002) Soil solution charge balance for defining the speed and time of centrifugation of two Brazilian soils. Commun Soil Sci Plant Anal 33:2021–2036. https://doi.org/10.1081/CSS-120005746

Phillips RP, Finzi AC, Bernhardt ES (2011) Enhanced root exudation induces microbial feedbacks to N cycling in a pine forest under long-term CO_2 fumigation. Ecol Lett 14:187–194. https://doi.org/10.1111/j.1461-0248.2010.01570.x

Rewald B, Rechenmacher A, Godbold DL (2014) It's complicated: Intraroot system variability of respiration and morphological traits in four deciduous tree species. Plant Physiol 166:736–745. https://doi.org/10.1104/pp.114.240267

Sasse J, Martinoia E, Northen T (2018) Feed your friends: do plant exudates shape the root microbiome? Trends Plant Sci 23:25–41. https://doi.org/10.1016/j.tplants.2017.09.003

Shang C, Zelazny LWW (2015) Selective dissolution techniques for mineral analysis of soils and sediments. In: Ulery AL, Drees LR (Eds.), Methods of soil analysis. Part 5. Mineralogical methods. Soil Sci Soc Am, Madison, WI, pp 33–80. https://doi.org/10.2136/sssabookser5.5.c3

Silva IR, Novais RF, Jham GN, Barros NF, Gebrim FO, Nunes FN, Neves JCL, Leite FP (2004) Responses of eucalypt species to aluminum: the possible involvement of low molecular weight organic acids in the Al tolerance mechanism. Tree Physiol 24:1267–1277. https://doi.org/10.1093/treephys/24.11.1267

Sokol NW, Bradford MA (2018) Microbial formation of stable soil carbon is more efficient from belowground than aboveground input. Nat Geosci 12:46–53. https://doi.org/10.1038/s41561-018-0258-6

Sterkenburg E, Clemmensen KE, Ekblad A, Finlay RD, Lindahl BD (2018) Contrasting effects of ectomycorrhizal fungi on early and late stage decomposition in a boreal forest. ISME J 12:2187–2197. https://doi.org/10.1038/s41396-018-0181-2

Sun GX, Chen SC, Li G, Li XM, Ding LJ, Reid BJ, Ciais P, Zhu YG (2021) The co-evolution of life and organics on earth: expansions of energy harnessing. Crit Rev Env Sci Technol 51:603–625. https://doi.org/10.1080/10643389.2020.1734434

Tavi NM, Martikainen PJ, Lokko K, Kontro M, Wild B, Richter A, Biasi C (2013) Linking microbial community structure and allocation of plant-derived carbon in an organic agricultural soil using $^{13}CO_2$ pulse-chase labelling combined with ^{13}C-PLFA profiling. Soil Biol Biochem 58:207–215. https://doi.org/10.1016/j.soilbio.2012.11.013

Teixeira PPC, Vidal A, Teixeira APM, Souza IF, Hurtarte LCC, Silva DHS, Almeida LFJ, Buegger F, Hammer EC, Jansa J, Mueller CW, Silva IR (2024) Decoding the rhizodeposit-derived carbon's journey into soil organic matter. Geoderma 443:116811. https://doi.org/10.1016/j.geoderma.2024.116811

Terrer C, Vicca S, Stocker BD, Hungate BA, Phillips RP, Reich PB, Finzi AC, Prentice IC (2018) Ecosystem responses to elevated CO_2 governed by plant-soil interactions and the cost of nitrogen acquisition. New Phytol 217:507–522. https://doi.org/10.1111/nph.14872

Valverde-Barrantes OJ, Freschet GT, Roumet C, Blackwood CB (2017) A worldview of root traits: the influence of ancestry, growth form, climate and mycorrhizal association on the functional trait variation of fine-root tissues in seed plants. New Phytol 215:1562–1573. https://doi.org/10.1111/nph.14571

Wang X, Chen R, Petropoulos E, You B, Lin X, Feng Y (2023) Root-derived C distribution drives N transport and transformation after ^{13}C and ^{15}N labelling on paddy and upland soils. Biol Fertil Soils 59:513–525. https://doi.org/10.1007/s00374-022-01681-6

Weemstra M, Mommer L, Visser EJW, van Ruijven J, Kuyper TW, Mohren GMJ, Sterck FJ (2016) Towards a multidimensional root trait framework: a tree root review. New Phytol 211:1159–1169. https://doi.org/10.1111/nph.14003

Wenzel WW, Wieshammer G, Fitz WJ, Puschenreiter M (2001) Novel rhizobox design to assess rhizosphere characteristics at high spatial resolution. Plant Soil 237:37–45. https://doi.org/10.1023/A:1013395122730

Willers C, van Jansen PJ, Claassens S (2015) Phospholipid fatty acid profiling of microbial communities-a review of interpretations and recent applications. J Appl Microbiol 119:1207–1218. https://doi.org/10.1111/jam.12902